

SAR and X-ray structures of enantiopure 1,2-*cis*-(1*R*,2*S*)-cyclopentyldiamine and cyclohexyldiamine derivatives as inhibitors of coagulation Factor Xa

Jennifer X. Qiao,* Chong-Hwan Chang, Daniel L. Cheney, Paul E. Morin, Gren Z. Wang, Sarah R. King, Tammy C. Wang, Alan R. Rendina, Joseph M. Luetzgen, Robert M. Knabb, Ruth R. Wexler and Patrick Y. S. Lam

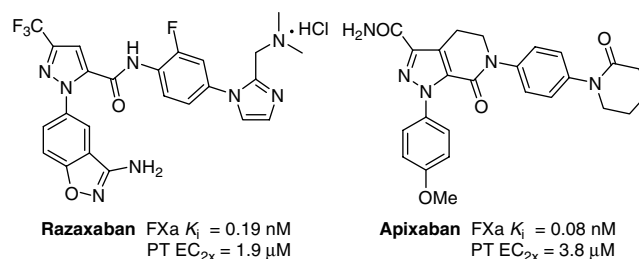
Bristol-Myers Squibb Company, Research and Development, PO Box 5400, Princeton, NJ 08543-5400, USA

Received 11 May 2007; revised 3 June 2007; accepted 5 June 2007
Available online 10 June 2007

Abstract—In the search of Factor Xa (FXa) inhibitors structurally different from the pyrazole-based series, we identified a viable series of enantiopure *cis*-(1*R*,2*S*)-cycloalkyldiamine derivatives as potent and selective inhibitors of FXa. Among them, cyclohexyldiamide **7** and cyclopentyldiamide **9** were the most potent neutral compounds, and had good anticoagulant activity comparable to the pyrazole-based analogs. Crystal structures of **7**-FXa and **9**-FXa illustrate binding similarities and differences between the five- and the six-membered core systems, and provide rationales for the observed SAR of P1 and linker moieties.
© 2007 Elsevier Ltd. All rights reserved.

Coagulation factor Xa (FXa), a serine protease positioned at the convergence of the intrinsic and the extrinsic pathways in the coagulation cascade, is an attractive target for developing novel, orally active anticoagulants for the treatment and prevention of thrombotic diseases. Selective FXa inhibitors might be more efficacious, have fewer bleeding risks, and a more favorable safety/efficacy ratio compared with thrombin inhibitors.^{1–3} Several small-molecule, orally active FXa inhibitors, including pyrazole-based razaxaban⁴ and apixaban,⁵ have entered clinical development, and apixaban is undergoing evaluation in phase 3 studies in various indications.

During the search for diverse scaffolds for FXa inhibition, compound **1** (Table 1) was identified as a lead bearing a simple ethylene diamine core with a *N*-phenylpyridone P4 group. The phenylpyridone group, as the unsaturated derivative of the phenylpiperidinone group found in apixaban,⁵ was a potent P4 moiety in the pyrazole-based series.⁶ Compound **1** showed good in vitro



FXa potency in the binding assay and modest anticoagulant activity in the prothrombin time (PT) assay (FXa K_i = 1.5 nM, PT EC_{2x} = 6.3 μ M), and was inactive against all the other serine proteases tested (trypsin, thrombin, urokinase, plasmin, aPC, tPA, plasma kallikrein, and chymotrypsin).

Figure 1 depicts the X-ray structure of the **1**-FXa complex with $R = 0.24$ at 1.8 Å resolution.⁷ In this complex, **1** adopts an L-shaped conformation, similar to that observed in the pyrazole-based analogs previously disclosed,^{4,5} with the chlorothiophene group occupying the S1 pocket and the phenylpyridone group bound to the S4 pocket. The P1 amide is coplanar with the thiophene ring, while the P4 amide is slightly tilted from the phenyl ring.

Keywords: Factor Xa inhibitors; (1*R*,2*S*)-cycloalkyldiamine derivatives; SAR; X-ray structure.

* Corresponding author. Fax: +1 609 818 6810; e-mail: jennifer.qiao@bms.com

Table 1. In vitro Xa potency of methyl-substituted ethylenediamine derivatives bearing a phenylpyridone P4 group

Compound	P1	R ¹	R ²	R ³	R ⁴	FXa K _i (nM)	PT EC _{2x} (μM)
1	A	H	H	H	H	1.5	6.3
1a (±)	A	Me	H	H	H	1.7	7.5
1b	A	Me	Me	H	H	3.2	nd
1c (±)	A	H	H	Me	H	2.1	12
1d	A	H	H	Me	Me	2.5	nd
2	B	H	H	H	H	13	nd
2a (±)	B	Me	H	H	H	10	nd
2b	B	Me	Me	H	H	1.3	17
2c (±)	B	H	H	Me	H	3.9	11
2d	B	H	H	Me	Me	4.8	nd

Purified human enzymes were used. Values were averages from multiple determinations ($n \geq 2$). K_i values were measured as described in Ref. 10. PT EC_{2x} (the concentration of the inhibitor that doubles the prothrombin time from the control) values were measured according to Ref. 4. Same for all tables.

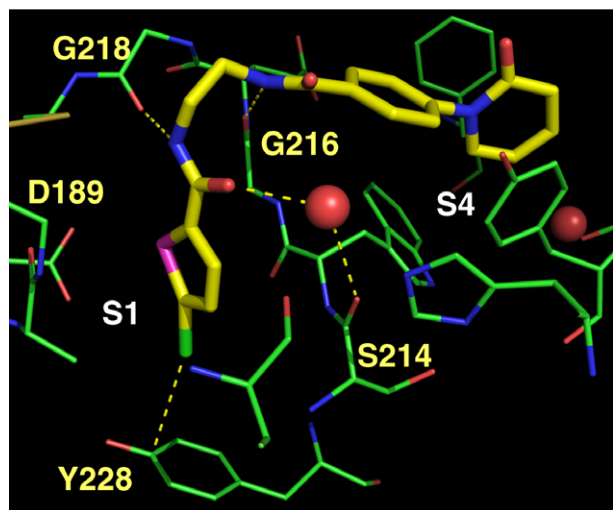


Figure 1. Interactions between compound **1** and the FXa active site. There is a water-mediated hydrogen-bond system involving the P1 carbonyl and Ser214 O. The P1 amide NH forms a hydrogen bond with Gly218 O, and the P4 amide NH forms a tight hydrogen bond with Gly216 O. The P1 Cl substituent forms a close contact with Tyr228 side chain.

S1 and S4 pockets are well-defined and distinctive subsites of FXa. Based on experience, we believe that interactions of a ligand in the FXa S1 and S4 subsites are essential to the FXa binding affinity of the ligand. The proper orientation of the P1 and P4 groups toward the S1 and S4 pockets could be achieved by the selection of an appropriate core or linker. The well-defined electron density of the flexible ethylene linker in the crystal structure of the **1**-FXa complex (Fig. 2) led us to the strategy of improving FXa binding affinity by adding one or more methyl groups on the ethylene linker to further stabilize the observed gauche conformation. The potency of the resulting methylated ethylenediamides is shown in Table 1. Adding methyl group(s) at either the C1 or the C2 position of the ethylene chain in **1** with

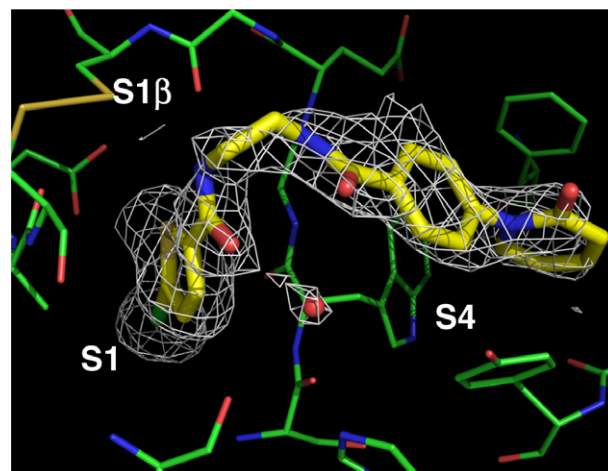
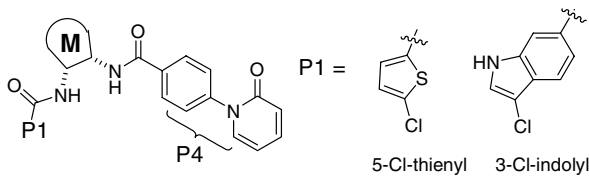


Figure 2. Compound **1** is shown with the initial $2F_o - F_c$ electron density map contoured at 0.7σ in white mesh. Created using PyMol.⁸

a 5-chlorothiophene P1 group (**A**) resulted in compounds having similar FXa inhibitory activity. In contrast, adding methyl group(s) in **2** bearing a larger bicyclic 3-chloroindole P1 group (**B**) resulted in improved anti-FXa activity (**2a–2d**). Compound **2b** with a gem-dimethyl substitution at C1 of the ethylene linker was 10-fold more active than the unsubstituted **2**. Modeling studies⁹ suggested that FXa potency could be further improved by modifying the methyl substituents in **2b** to interact with the disulfide bridge region (S1β). We did not investigate this series further due to the negligible solubility and relatively low anticoagulant activity of **2b**, the latter of which is suggestive of high protein binding.

Another way of constraining the floppy ethylene linker in **1** and **2** is to tie back the C1 and the C2 CH₂ groups to form cyclicdiamine derivatives (Table 2). We found that the *cis* racemic cyclohexyl analogs **3** and **5** were slightly (threefold) more active than the *trans* analogs

Table 2. Stereochemistry of cycloalkyldiamine derivatives bearing a phenylpyridone P4 group


Compound	M	Stereochemistry	P1	FXa K_i (nM)
1		—	5-Cl-thienyl	1.5
2		—	3-Cl-indolyl	13
3		<i>cis</i> -(±)	3-Cl-indolyl	1.0
4		<i>trans</i> -(±)	3-Cl-indolyl	3.7
5		<i>cis</i> -(±)	5-Cl-thienyl	7.3
6		<i>trans</i> -(±)	5-Cl-thienyl	23
7		(1 <i>R</i> , 2 <i>S</i>)	3-Cl-indolyl	0.67
8		(1 <i>S</i> , 2 <i>R</i>)	3-Cl-indolyl	3.8
9		(1 <i>R</i> , 2 <i>S</i>)	5-Cl-thienyl	0.43
10		(1 <i>S</i> , 2 <i>R</i>)	5-Cl-thienyl	87

4 and 6, respectively. The cyclohexyldiamine derivative 7 (FXa K_i = 0.67 nM) bearing a 3-chloroindole P1 group with a *cis*-(1*R*,2*S*) configuration was five times more potent than its enantiomer 8, and the *cis* cyclopentyldiamine derivative 9 (FXa K_i = 0.43 nM) bearing a 5-chlorothiophene P1 group with the same (1*R*,2*S*) configuration was 200-fold more potent than its enantiomer 10. Compounds 9 and 7 were threefold and 20-fold more potent than the corresponding ethylenediamine leads 1 and 2, respectively. The absolute stereochemistry of 9, *cis*-(1*R*,2*S*), was confirmed by single crystal X-ray analysis¹¹ using the anomalous dispersion of sulfur and chlorine atoms. Given the potency of the *cis* analogs, the SAR discussion reported herein will therefore focus on the *cis*-(1*R*,2*S*)-cyclopentyldiamine and *cis*-(1*R*,2*S*)-cyclohexyldiamine core systems.

P1 SAR of (1*R*,2*S*)-cyclopentyldiamine and (1*R*,2*S*)-cyclohexyldiamine derivatives bearing phenylpyridone P4 group. In the cyclopentyldiamine series (Table 3), 9 with a 5-chlorothiophene group was the most potent among compounds bearing monocyclic P1 groups, and it was 80-fold more potent than the 4-chlorophenyl analog

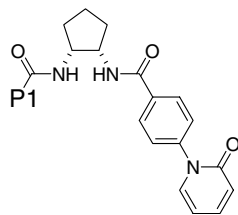
17. Compound 11 with a 3-chloroindole group was the most potent among compounds bearing chlorinated bicyclic (hetero) aromatic P1 groups (11–16).

Adding a nitrogen in the thiophene ring of 9 resulted in more than three orders of magnitude loss of potency (18). Chlorine substitution and the position of the chlorine are essential to the compound's FXa inhibitory activity.¹² Replacing the chlorine atom with a methyl group (9 vs 19), or a methoxy group (17 vs 20), and removing the chlorine atom (11 vs 21) resulted in five-fold to 120-fold decrease of potency. The 4-Cl-phenyl analog 17 was 30-fold and 70-fold more potent than the 3- and 2-Cl-phenyls (22, 23), respectively. *Ortho*- or *meta*-substitution on the 4-chlorophenyl ring in 17 with F, Cl, OMe, Me, and SO₂Me resulted in decreased FXa potency (22–32).

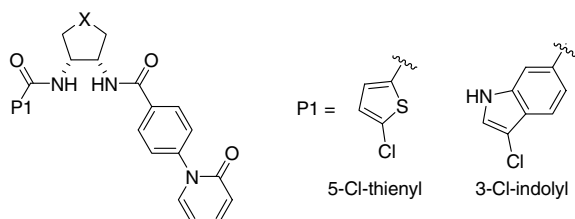
5-Chlorothiophene and 3-chloroindole in 9 and 7 were the two best P1 groups in both the five- and the six-membered core series (Table 4). 6-Chloronaphthyl, 6-chlorobenzo[*b*]thiophenyl, and 4-chlorophenyl P1 groups provided compounds that were one to two orders of magnitude less active than 9 and 7. Tables 3 and 4 show that subtle structural deviations from 5-chlorothiophene and 3-chloroindole P1 groups reduced FXa potency drastically, revealing the importance of the S1 pocket of serine proteases for binding affinity.

P4 SAR of (1*R*,2*S*)-cyclopentyldiamine and (1*R*,2*S*)-cyclohexyldiamine derivatives. FXa activities of (1*R*,2*S*)-cyclopentyl and cyclohexyldiamine core systems containing a variety of P4 groups were studied using 5-chlorothiophene and 3-chloroindole P1 groups (Table 5). Pyridones 7, 9, and 11 and α -CH₂-*N*-pyrrolidinyl phenylcyclopropyl analogs 54–56 were the most potent FXa inhibitors (FXa K_i ≤ 1 nM) in both core systems. Compounds containing a variety of six-membered lactam-based P4 moieties, such as piperidinones 40–42, morpholinone 43, cyclic carbamate 44, and cyclic urea 45, were potent with K_i values less than 5 nM. The basic 2-dimethylaminomethyl imidazole 50 and piperidinone 42 were also similar in potency. Compounds 46 and 47 bearing five- and seven-membered lactam P4 groups were less potent than piperidinones 40–42. The cyclic sulfonamide in 48 was the least potent P4 group in this study.

Table 5 shows that cyclohexyldiamine derivatives bearing the larger 3-chloroindole P1 group were slightly more potent than the cyclopentyldiamine counterparts. For example, compounds 7, 50, and 54 were two- to fivefold more potent than compounds 11, 49, and 53, respectively. In contrast, when using the smaller 5-chlorothiophene P1 group, the resulting cyclopentyldiamine derivatives were equal or slightly more potent than the corresponding cyclohexyldiamines (9 vs 37, fourfold; 55 vs 56, twofold; and 51 vs 52, twofold). Most compounds with good binding activity (FXa K_i < 2 nM) also demonstrated good anticoagulant activity in the clotting time functional assay. Compared with pyrazole-based raxazaban⁴ and apixaban,⁵ these cyclic diamides were less potent in FXa binding affinity (FXa K_i). However,

Table 3. P1 SAR of (1*R*,2*S*)-cyclopentylidiamine derivatives bearing a phenylpyridone P4 group

Compound	P1	FXa K_i (nM)
9	5-Cl-2-thienyl	0.43
11	3-Cl-6-indolyl	1.0
12	5-Cl-2-indolyl	74
13	6-Cl-2-indolyl	266
14	6-Cl-2-benzo[<i>b</i>]thiophenyl	34
15	5-Cl-2-benzo[<i>b</i>]thiophenyl	288
16	6-Cl-2-naphthyl	27
17	4-Cl-phenyl	36
18	2-Cl-5-thiazolyl	1220
19	5-Me-2-thienyl	7.92
20	4-MeO-phenyl	170
21	6-Indolyl	124
22	3-Cl-phenyl	1186
23	2-Cl-phenyl	2610
24	4-Cl-3-Me-phenyl	138
25	4-Cl-3-OMe-phenyl	892
26	4-Cl-3-F-phenyl	226
27	3,4-di-Cl-phenyl	433
28	4-Cl-2-F-phenyl	129
29	2,4-di-Cl-phenyl	360
30	4-Cl-2-Me-phenyl	603
31	4-Cl-2-MeO-phenyl	7420
32	4-Cl-2-SO ₂ Me-phenyl	8560

Table 4. P1 SAR of cyclopentylidiamine vs cyclohexylidiamine derivatives bearing a phenylpyridone P4 group

Compound	P1	X	FXa K_i (nM)
11	3-Cl-6-indolyl	-CH ₂ -	1.0
7	3-Cl-6-indolyl	-CH ₂ CH ₂ -	0.67
13	6-Cl-2-indolyl	-CH ₂ -	266
33	6-Cl-2-indolyl	-CH ₂ CH ₂ -	14
14	6-Cl-2-benzo[<i>b</i>]thiophenyl	-CH ₂ -	34
34	6-Cl-2-benzo[<i>b</i>]thiophenyl	-CH ₂ CH ₂ -	16
16	6-Cl-2-naphthyl	-CH ₂ -	27
35	6-Cl-2-naphthyl	-CH ₂ CH ₂ -	20
17	4-Cl-phenyl	-CH ₂ -	36
36	4-Cl-phenyl	-CH ₂ CH ₂ -	37
9	5-Cl-2-thienyl	-CH ₂ -	0.43
37	5-Cl-2-thienyl	-CH ₂ CH ₂ -	1.8

the most potent compounds such as **7**, **9**, **38**, **40**, **54–56** showed comparably good anticoagulant activity (PT EC_{2x} 2–3 μM) in human plasma, which we assume to

be the result of the reduced lipophilicity, which in turn lowers protein binding.

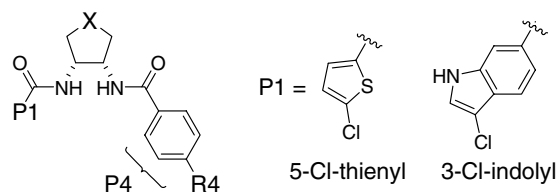
In general, the series of compounds in **Table 5** were highly selective against other related serine proteases (see **Table 6** for four representative compounds). The observed high selectivity resulted from the structural variations in the S1 and S4 pockets of the different serine proteases (e.g., the size difference of the S4 pockets, the Ala190Ser difference in the S1 pockets), evident in the overlay of the publicly available crystal structures.

Linker SAR. **Tables 7 and 8** list FXa potency of five- and six-membered cores with different P1 and P4 linkers. Compounds **7** and **9** with P1 and P4 amide linkers were the most potent. Compounds with a planar P1 linker, such as amides **9** and **17**, urea **57**, and oxalamide **58**, were much more potent than those with an aplanar linker, such as methylamine **59** and sulfonamide **60**. Changing the P4 amide in **7** to a sulfonamide in **63** led to loss of potency, while the methylsulfonyl P4 linker analog **64** (racemic) resulted in 19-fold loss of potency. Different SAR of P4 linker was observed between the five- and six-membered core systems: in the five-membered core, reducing the P4 amide in **9** to a methylamine in **61** led to 10-fold loss of potency; while in the six-membered ring system, the corresponding methylamine **65** had similar FXa potency as parent **7**. *Ortho* substitution on the inner phenyl ring in cyclopentyl **9** with a fluorine atom in **62** resulted in a 10-fold drop of FXa potency; while for the six-membered ring, FXa potency of the fluorine analog **66** was maintained compared with **7**.

X-ray structures of compounds 7 and 9. Cyclopentyl-diamide **9** with a chlorothiophene P1 and cyclohexyl-diamide **7** with a chloroindole P1 were the most potent neutral leads in this series. X-ray crystal structures of **7**-FXa¹³ and **9**-FXa¹⁴ complexes were obtained with resolution at 2.2 Å and 1.8 Å, respectively. **Figures 3 and 4** illustrate the interactions of **7** and **9**, respectively, with the FXa residues in the active site. **Figure 5** shows the overlay of the X-ray structures of FXa-bound ethylene-diamide **1**, cyclohexylidiamide **7**, and cyclopentylidiamide **9**. All three molecules bind in a similar extended manner, with the chloroheteroaryl groups occupying the S1 pocket and the phenylpyridone group bound to the S4 pocket. The pyridone ring in each of the three molecules forms an edge-to-face interaction with Tyr215, and stacks nicely between Tyr99 and Phe174.

The chlorothiophene groups of **1** and **9** and the chloroindole group of **7** are buried deeply inside the S1 pocket (**Fig. 5**). The chlorine atoms occupy essentially the same position at the bottom of the S1 pocket, displacing a structurally conserved water and forming close contacts with Tyr228. The average Cl···Tyr228CZ distance is 3.6 Å. Such Cl–Tyr228 interaction (presumably Ar–Cl···π interaction) is also observed in other inhibitor-FXa complexes.¹² The narrow P1 SAR could be at least partially attributed to the high degree of directional preference¹⁵ of the Ar–Cl···π interactions. The overall conformation of the cyclopentylidiamide **9** is very similar

Table 5. P4 SAR of cyclopentyl- and cyclohexyl-diamine derivatives



Compound	P4	P1	X	FXa K_i (nM)	PT EC_{2x} (μM)
9		5-Cl-thienyl	$-\text{CH}_2-$	0.43	1.7 (aPTT = 3.6)
37		5-Cl-thienyl	$-\text{CH}_2\text{CH}_2-$	1.8	6.5
11		3-Cl-indolyl	$-\text{CH}_2-$	1.0	5.5
7		3-Cl-indolyl	$-\text{CH}_2\text{CH}_2-$	0.67	3.2 (aPTT = 4.4)
38		5-Cl-thienyl	$-\text{CH}_2-$	1.1	2.3
39		3-Cl-indolyl	$-\text{CH}_2\text{CH}_2-$	0.94	6.0
40		5-Cl-thienyl	$-\text{CH}_2-$	1.5	3.5
41		3-Cl-indolyl	$-\text{CH}_2-$	2.6	nd
42		3-Cl-indolyl	$-\text{CH}_2\text{CH}_2-$	2.6	nd
43		3-Cl-indolyl	$-\text{CH}_2-$	4.2	nd
44		3-Cl-indolyl	$-\text{CH}_2\text{CH}_2-$	5.0	nd
45		3-Cl-indolyl	$-\text{CH}_2\text{CH}_2-$	4.0	nd
46		3-Cl-indolyl	$-\text{CH}_2\text{CH}_2-$	8.1	nd
47		3-Cl-indolyl	$-\text{CH}_2\text{CH}_2-$	17	nd
48		3-Cl-indolyl	$-\text{CH}_2\text{CH}_2-$	107	nd

(continued on next page)

Table 5 (continued)

Compound	P4	P1	X	FXa K_i (nM)	PT EC_{2x} (μ M)
49		3-Cl-indolyl	-CH ₂ -	7.1	nd
50		3-Cl-indolyl	-CH ₂ CH ₂ -	2.3	nd
51		5-Cl-thienyl	-CH ₂ -	2.8	nd
52		5-Cl-thienyl	-CH ₂ CH ₂ -	4.4	nd
53		3-Cl-indolyl	-CH ₂ -	2.4	10
54		3-Cl-indolyl	-CH ₂ CH ₂ -	0.44	2.8
55		5-Cl-thienyl	-CH ₂ -	0.51	2.1
56		5-Cl-thienyl	-CH ₂ CH ₂ -	0.95	2.9
Raxazaban				0.19	1.9
Apixaban				0.08	3.8

Table 6. Human enzyme selectivity profile

Enzyme K_i (nM)	7	9	40	55
FXa	0.67	0.43	1.5	0.51
Thrombin	>12,000	7660	8871	3601
Trypsin	>5000	>5000	>5000	>5000
Factor VIIa	>16,000	>16,000	>10,000	>10,000
Factor XIa	>15,000	>15,000	>10,000	>10,000
aPC	>21,000	>21,000	>21,000	>21,000
Plasmin	>22,000	>22,000	>22,000	>22,000
tPA	5502	>20,000	>20,000	>20,000
Urokinase	>14,000	>14,000	>14,000	>14,000
Plasma kallikrein	8458	>16,000	>10,000	>10,000
Chymotrypsin	>20,000	>20,000	>20,000	>20,000

All K_i 's were obtained from purified human enzymes and were averaged from multiple determinations ($n \geq 2$). See Ref. 4 for more details.

Table 7. Linker SAR of *cis*-cyclophenyl core system

Compound	P1	P1 linker (G)	P4 linker (Z)	R ¹	FXa K_i (nM)
9	5-Cl-thienyl	-CONH-	-NHCO-	H	0.43
17	4-Cl-phenyl	-CONH-	-NHCO-	H	36
57	4-Cl-phenyl	-NHCONH-	-NHCO-	H	10
58	5-Cl-pyridinyl	-NHCOCONH-	-NHCO-	H	9.9
59	5-Cl-thienyl	-CH ₂ NH-	-NHCO-	H	82
60	4-Cl-phenyl	-SO ₂ NH-	-NHCO-	H	11500
61	5-Cl-thienyl	-CONH-	-NHCH ₂ -	H	4.2
62	5-Cl-thienyl	-CONH-	-NHCO-	F	4.7

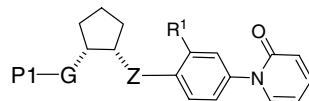
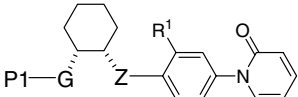


Table 8. Linker SAR of *cis*-cyclohexyl system


Compound	P1	P1 linker (G)	P4 linker (Z)	R ¹	FXa K _i nM
7	3-Cl-indolyl	-CONH-	-NHCO-	H	0.67
63	3-Cl-indolyl	-CONH-	-NHSO ₂ -	H	929
64 (±)	3-Cl-indolyl	-CONH-	-CH ₂ SO ₂ -	H	13
65	3-Cl-indolyl	-CONH-	-NHCH ₂ -	H	1.3
66	3-Cl-indolyl	-CONH-	-NHCO-	F	0.71

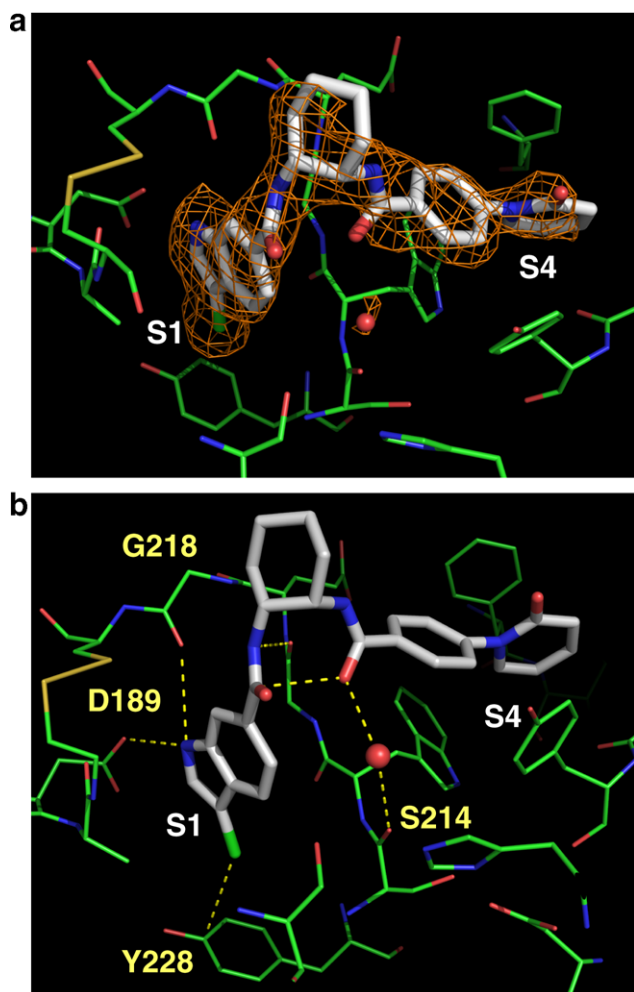


Figure 3. (a) Compound 7 is shown with the initial $2F_o - F_c$ electron density map contoured at 1σ in orange mesh. The electron density for the putative water involved in hydrogen bonding to S214 is contoured at 0.8σ . Created using PyMol.⁸ (b) Interactions between cyclohexyl analog 7 and the FXa active site. The P1 amide NH forms a weak hydrogen bond with Gly216 O, and the P4 amide O forms a water mediated hydrogen bond with Ser214 O. The NH of the indole ring forms a hydrogen bond with Asp189 O and with Gly218 O, respectively. The cyclohexyl ring adopts a chair form. The P1 Cl substituent forms a close contact with Tyr228 side chain.

to that of the ethylenediamide **1**, which shares the same P1 group with **9**. However, the thiophene ring in **9** is rotated 180 degrees from that in **1**, keeping the

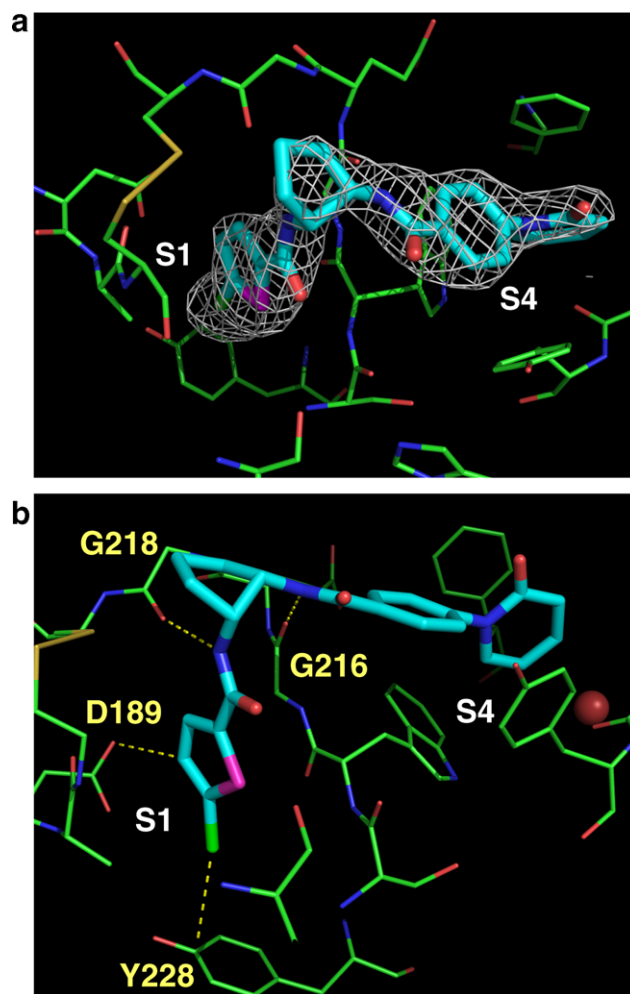


Figure 4. (a) Compound **9** is shown with the initial $2F_o - F_c$ electron density map contoured at 1σ in white mesh. Created using PyMol.⁸ (b) Interactions between cyclopentyl analog **9** and the FXa active site. The P1 amide NH forms a weak hydrogen bond with Gly218 O; while the P4 amide NH forms a tight hydrogen bond to Gly216 O. C4-H of the thiophene ring forms a close contact with Asp189 side chain, presumably engaging in weak electrostatic interactions. The P1 Cl substituent forms a close contact with Tyr228 side chain.

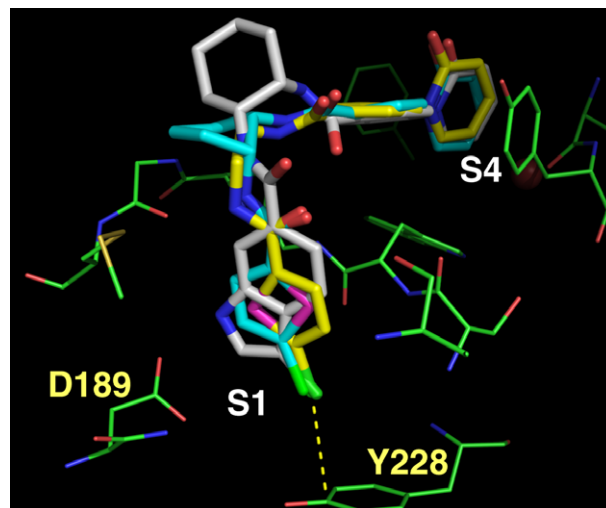
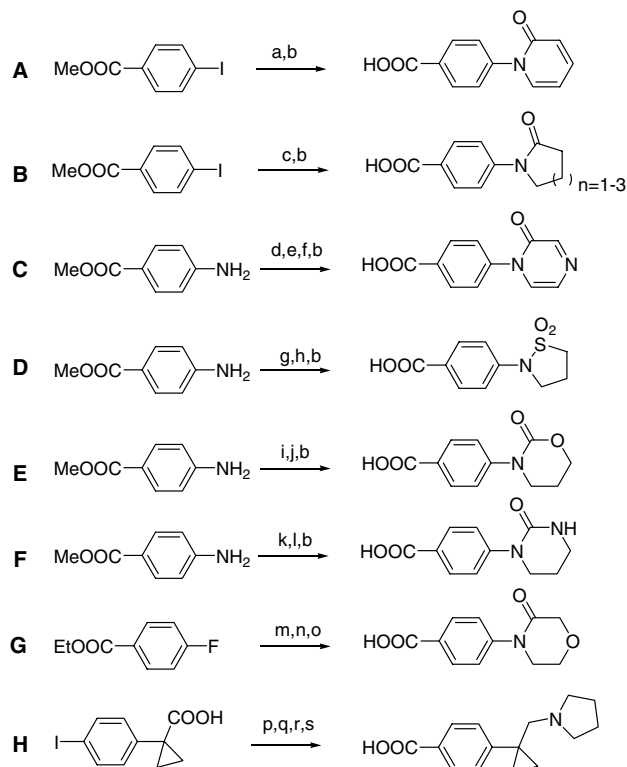


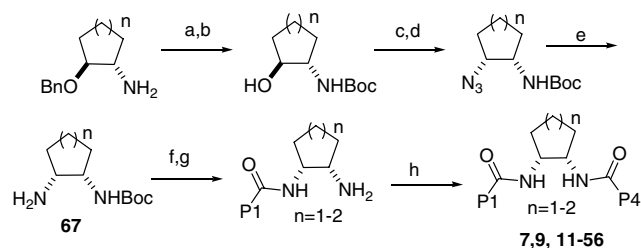
Figure 5. Overlay of X-ray structures of compounds **1** (yellow), **7** (white), and **9** (blue) in the active site of FXa.

chlorine atom at essentially the same position in the S1 pocket.

The overlay of the X-ray structures of **7-FXa** and **9-FXa** (Fig. 5) clearly shows significant binding differences in both the cycloalkyl core and the amide linker region of **7** and **9**, suggesting that different approaches may be needed to optimize the five- and the six-membered ring systems. The cyclohexyl ring in **7-FXa** with a preferred bicyclic indole P1 group locates farther away from the S1 pocket than the cyclopentyl ring in **9-FXa** bearing a smaller thiophene P1 group. Hydrogen bonding possibilities of the two amide linkers of **9** and **7** are different (see Figs. 3 and 4). In addition, the relative orientation of the two amides with their adjacent aromatic rings is different in these two compounds. In cyclopentyl **9**, the P1 amide is almost coplanar with the thiophene ring, and the P4 amide is nearly coplanar with the inner phenyl ring; while in cyclohexyl **7**, the two amides are not at the same plane as that of the indole or the inner



Scheme 1. Reagents and conditions: (a) 2-Hydroxypyridine, CuI, K_2CO_3 , 1,10-phenanthroline, 120 °C, overnight, 82%; (b) 1 N NaOH, MeOH, rt to 50 °C, 80%-quant.; (c) Five- to seven-membered lactams, K_2CO_3 , CuI, 1,10-phenanthroline, DMSO, 120–125 °C, overnight to 1 day, 25–80%; (d) Boc-Gly-OH, BOP, DIEA, DMF, rt, 1.5 h, 98%; (e) TFA, CH_2Cl_2 , rt, 1.5 h, quant.; (f) Glyoxal (40% aq), NaOH, H_2O , MeOH, –40 to 5 °C, 3 h, 55%; (g) [1,2]Oxathiolane 2,2-dioxide, neat, 110 °C, 1 h, 71%; (h) $POCl_3$, reflux, 105 °C, 4 h; then 4 N NaOH, 94%; (i) $ClCOO(CH_2)_3Cl$, THF, 0 °C to rt, 2 h; (j) NaH, THF, 0 °C, 3 h, 47% for 2 steps; (k) $Cl(CH_2)_3NCO$, THF, rt overnight; (l) NaH, THF, rt, 3.5 h, 50% for 2 steps; (m) morpholine (3.3 equiv), 120 °C, neat, 2 day, 96%; (n) $KMnO_4$, $PhCH_2N^+Et_3Cl^-$, CH_2Cl_2 , 50 °C, 3 h, 59%; (o) 1 N NaOH, EtOH, 89%; (p) $ClCOEt$, Et_3N , CH_2Cl_2 , 0 °C, 30 min; $NaBH_4$, MeOH, 0 °C, 30 min; (q) NaOAc, PCC, 4 Å MS, CH_2Cl_2 , rt, 1.5 h; (r) pyrrolidine, $NaBH(OAc)_3$, HOAc, CH_2Cl_2 , rt, 20 min, 41% for 3 steps; (s) KOAc, $Pd(OAc)_2$, dppe, DMF/ H_2O , CO, 60 °C, 2.5 h, 90%.



Scheme 2. Reagents and conditions: (a) Boc_2O , Et_3N , THF, quant.; (b) Pd-C (5%), H_2 (25 psi), EtOH, 6 h, 96%; (c) MsCl, Et_3N , CH_2Cl_2 , 0 °C, 2 h, 92%; (d) NaN_3 , DMF, 80 °C, overnight; (e) Pd-C (10%), H_2 , EtOH, 6 h, 40% for two steps; (f) P1-COOH, HATU, DIEA, DMF, 54% (for 5-chlorothiophene-2-COOH), 62% (for 3-chloroindole-6-COOH); (g) TFA, CH_2Cl_2 ; (h) P4-COOH, BOP, NMM, DMF, or HATU, DIEA, DMF, 10–90% for two steps.

phenyl ring. This suggests that the amide linker region in the cyclopentyl core system may be less tolerable to structural changes than those in the cyclohexyl core system.

Synthesis. Schemes 1 and 2 outline the synthesis of enantiopure *cis*-(1*R*,2*S*)-cyclopentyl and cyclohexyl-diamine derivatives bearing a variety of P4 groups. The requisite P4 acids were synthesized according to the straightforward transformations illustrated in sequences A to H (Scheme 1). The Boc-protected cyclic diamine cores **67** were prepared from commercially available enantiopure benzyl protected amino alcohols via a sequence of deprotection, mesylation, azide displacement, and then reduction of the azide. Two subsequent amide formation reactions of the P4 and the P1 acids with cores **67** generated the desired products (Scheme 2).

In summary, using both structure-based design and traditional medicinal chemistry approaches, we identified enantiopure *cis*-(1*R*,2*S*)-cycloalkyl diamine derivatives as a viable series of potent, selective FXa inhibitors that are structurally different from previously reported pyrazole-based scaffolds. The 5-chlorothiophene and 3-chloroindole P1 groups were identified as potent P1 fragments for FXa inhibition in this series. Example compounds bearing a variety of *N*-phenyl substituted lactam-based P4 groups and α - CH_2 -*N*-pyrrolidinyl-phenylcyclopropyl P4 group showed excellent binding affinity (<1 nM), good potency in human plasma clotting assay (<5 μ M), and high selectivity against other serine proteases (>5000-fold). Among them, the cyclopentyl-diamide **9** and the cyclohexyldiamide **7** were the most potent neutral analogs with anticoagulant activity comparable to raxazaban and apixaban. In each of the X-ray structures of FXa-bound **9** and **7**, the P1 group sits deep in the S1 subsite and there exist interactions between the chlorine and Tyr228. The crystal structures of **7-FXa** and **9-FXa** complexes provided insights to guide further structural optimization of the cyclic diamine derivatives to modulate *in vitro* and *in vivo* properties, which shall be reported in future communications.

Acknowledgments

The authors thank Dr. Steven Sheriff for depositing **1-FXa**, **7-FXa**, and **9-FXa** complexes into PDB, Qi Gao and Dedong Wu for single crystal X-ray structure determination of **9**, and Jeffrey M. Bozarth, Frank A. Barbera, Tracy A. Bozarth, and Karen S. Hartl for performing in vitro assays.

References and notes

- Part of this research was presented at the 232nd ACS National Meeting, San Francisco, CA, September 10–14, 2006, MEDI-393.
- For recent review papers of FXa inhibitors, see: (a) Quan, M.; Smallheer, J. *Curr. Opin. Drug Discov. Devel.* **2004**, *7*, 460; (b) Walenga, J. M.; Jeske, W. P.; Hoppensteadt, D.; Fareed, J. *Curr. Opin. Investig. Drugs* **2003**, *4*, 272; (c) Gould, W. R.; Leadley, R. J. *Curr. Pharm. Design* **2003**, *9*, 2337; (d) Quan, M. L.; Wexler, R. R. *Curr. Top. Med. Chem.* **2001**, *1*, 137.
- (a) Lassen, M. R.; Davidson, B. L.; Gallus, A.; Pineo, G.; Ansell, J.; Deitchman, D. *Blood* **2003**, *102*, 11; (b) Straub, A.; Pohlmann, J.; Lampe, T.; Pernerstorfer, J.; Schlemmer, K.-H.; Reinemer, P.; Perzborn, E.; Roehrig, S. *J. Med. Chem.* **2005**, *48*, 5900; (c) Eriksson, B. L.; Borris, L.; Dahl, O. E.; Haas, S.; Huisman, M. V.; Kakkar, A. K. *J. Thromb. Haemost.* **2006**, *4*, 121; (d) Hampton, T. *JAMA* **2006**, *295*, 743; (e) Wong, P. C.; Crain, E. J.; Watson, C. A.; Zaspel, A. M.; Wright, M. R.; Lam, P. Y. S.; Pinto, D. J.; Wexler, R. R.; Knabb, R. M. *J. Pharmacol. Exp. Ther.* **2002**, *303*, 993.
- Quan, M. L.; Lam, P. Y. S.; Han, Q.; Pinto, D. J.; He, M.; Li, R.; Ellis, C. D.; Clark, C. G.; Teleha, C. A.; Sun, J. H.; Alexander, R. S.; Bai, S. A.; Luetzgen, J. M.; Knabb, R. M.; Wong, P. C.; Wexler, R. R. *J. Med. Chem.* **2005**, *48*, 1729.
- Pinto, D. J. P.; Orwat, M. J.; Koch, S.; Rossi, K. A.; Alexander, R. S.; Smallwood, A.; Wong, P. C.; Rendina, R. A.; Luetzgen, J. M.; Knabb, R. M.; He, K.; Xin, B.; Wexler, R. R.; and Lam, P. Y. S. *J. Med. Chem.* Accepted for publication.
- Pinto, D.; Quan, M.; Orwat, M.; Li, Y.; Han, W.; Qiao, J.; Lam, P.; Koch, S. WO 2003026652 A1, 2003.
- PDB Deposition number for **1-FXa** complex is **2P93**.
- DeLano, W. L. The PyMOL Molecular Graphics System (2002) on World Wide Web <http://www.pymol.org>.
- Idea structures were evaluated with molecular dynamics using Discover_3 with the CFF98 forcefield within the InsightII v2000.L3 modeling software package. www.accelrys.com.
- (a) Knabb, R. M.; Kettner, C. A.; Timmermans, P. B. M. W. M.; Reilly, T. M. *Thromb. Haemost.* **1992**, *67*, 56; (b) Kettner, C. A.; Mersinger, L. J.; Knabb, R. M. *J. Biol. Chem.* **1990**, *265*, 18289.
- There are three crystallographically independent molecules having the same chirality in one asymmetric unit. Three molecules are bound together by hydrogen bonding between –NH and amide groups (N···O 2.917–3.128 Å), and solvent molecules (probably CH₂Cl₂ and H₂O) are disordering in the crystal lattice.
- (a) Adler, M.; Kochanny, M. J.; Ye, B.; Rummenik, G.; Light, D. R.; Biancalana, S.; Whitlow, M. *Biochemistry* **2002**, *41*, 15514; (b) Maignan, S.; Guilloteau, J.-P.; Choi-Sledeski, Y. M.; Becker, M. R.; Ewing, W. R.; Pauls, H. W.; Spada, A. P.; Mikol, V. *J. Med. Chem.* **2003**, *46*, 685; (c) Matter, H.; Will, D. W.; Nazaré, M.; Schreuder, H.; Laux, V.; Wehner, V. *J. Med. Chem.* **2005**, *48*, 3290; (d) Nazare, M.; Will, D. W.; Matter, H.; Schreuder, H.; Ritter, K.; Urmann, M.; Essrich, M.; Bauer, A.; Wagner, M.; Czech, J.; Lorenz, M.; Laux, V.; Wehner, V. *J. Med. Chem.* **2005**, *48*, 4511.
- PDB Deposition number for **7-FXa** complex is **2P94**.
- PDB Deposition number for **9-FXa** complex is **2P95**.
- Saraogi, Ishu.; Vijay, V. G.; Das, Soma; Sekar, K.; Row, T. N. *Crystal Eng.* **2003**, *6*, 69.